Deposition Mechanism and Microstructure of Laser-Assisted Cold-Sprayed (LACS) Al-12 wt.%Si Coatings: Effects of Laser Power

E.O. OLAKANMI,[1,4,5] M. TLOTLENG,[1,2] C. MEACOCK,[2] S. PITYANA,[2,3] and M. DOYOYO[1]

1.—Department of Mechanical Engineering Science, University of Johannesburg, Johannesburg 2006, South Africa. 2.—National Laser Centre, Council for Scientific and Industrial Research, Pretoria 0001, South Africa. 3.—Department of Chemical and Metallurgical Engineering, Tshwane University of Technology, Pretoria 0001, South Africa. 4.—Department of Mechanical Engineering, Federal University of Technology, P.M.B. 65, Minna, Nigeria. 5.—e-mail: eolakanmi@uj.ac.za

Surface treatment is one of the most costly processes for treating metallic components against corrosion. Laser-assisted cold spray (LACS) has an opportunity to decrease those costs particularly in transportation systems, chemical industries, and renewable energy systems. This article highlights some of those potential applications. In the LACS process, a laser beam irradiates the substrate and the particles, thereby softening both of them. Consequently, the particles deform upon impact at the substrate and build up a coating. To circumvent the processing problems associated with cold-spray (CS) deposition of low-temperature, corrosion-resistant Al-12 wt.%Si coatings, a preliminary investigation detailing the effect of laser power on its LACS deposition mechanism and microstructural properties is presented. The deposition efficiency, the microstructure, and the microhardness of the LACS-deposited coatings produced by a 4.4-kW Nd:YAG laser system were evaluated. The outcome of this study shows that pore- and crack-free Al-12 wt.%Si coatings were deposited via softening by laser irradiation and adiabatic shearing phenomena at an optimum laser power of 2.5 kW.

INTRODUCTION

The durability of engineering components is determined by their surface integrity when they encounter corrosion and wear in their operating environments. The application of corrosion- and wear-resistant coatings on these components is an effective way to improve their surface integrity in their service environments. The need arises for the development of cheap and easily processable coating materials (e.g., eutectic Al-12 wt.%Si alloy) with enhanced surface integrity, which has applications in transportation systems, chemical industries, and renewable energy systems. For instance, Al-12 wt.%Si alloy is employed for salvaging and building up of parts, repair of worn components, and dimensional restoration of mismachined parts in manufacture. The Si in the alloy imparts excellent fluidity, high strength, low thermal expansion coefficient, high thermal conductivity, and high wear resistance, and it decreases contraction associated with its solidification.[1,2]

Currently, the deposition of coatings is limited to processes using both traditional and thermal approaches of coating deposition. Although the traditional approaches (electroplating and chemical vapor deposition) are generally slow and expensive, thermally sprayed coating techniques (vacuum plasma spray, laser cladding, and high-velocity oxygen flame) are bedeviled with challenges such as component distortion, formation of undesirable intermetallic phases, poor mechanical properties, occurrence of high residual stresses, oxidation, and the requirement of high-purity inert environments to prevent oxidation during processing.[2–4] Moreover, fabrication of Al-12 wt.%Si alloy and its composites' coatings had been accomplished via several cycles with the necessity of optimizing each cycle to

Deposition Mechanism and Microstructure of Laser-Assisted Cold-Sprayed (LACS)
Al-12 wt.%Si Coatings: Effects of Laser Power
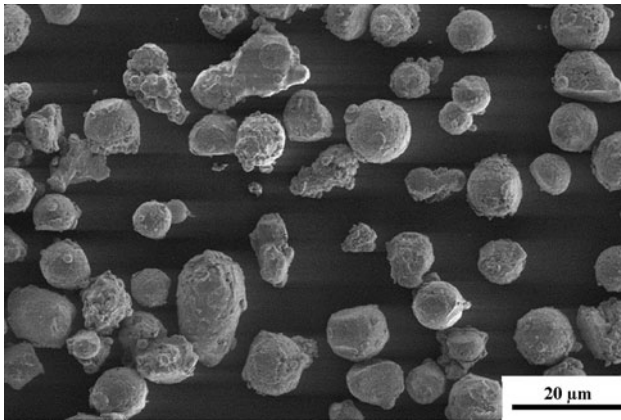
777

Fig. 1. Morphology of Al-12 wt.%Si powders used for this study.

match their performance requirements in service. It has also been acknowledged that the use of diverse equipment in processing coatings increases their cost and hinders the repeatability of their structure and properties.

To overcome the processing challenges of coatings highlighted above, several researchers have employed a nonmelting cold-spray (CS) process to deposit Al-Si alloy and its composites' coatings.[1,5–7] CS deposits coatings by entraining powder particles within a supersonic gas jet that accelerates before it impinges on the deposition site at high velocities. The severe plastic deformation of particles that is responsible for their bonding with the substrate and subsequent formation of coatings has been credited to the impact of the particles on the deposition site. This occurs at a velocity above a critical value depending on the powder properties and processing parameters.[1,5,6] Nevertheless, problems are also associated with CS deposition of Al-12 wt.%Si coatings and other materials. These problems include high operating costs accrued from gas consumption and heating. Moreover, bond strength and density are reduced when depositing hard materials, and the coatings generally have large compressive residual stresses. In summary, high operating costs and a limited range of materials have restricted the number of applications for which CS is economically viable.[8,9]

To address the problems associated with CS deposition of Al-12 wt.%Si coatings, the application of a relatively new laser-assisted cold-spray (LACS) process is hereby extended to the deposition of its coatings by using cheaper nitrogen gas, thereby eliminating the need for expensive helium gas as well as gas heating. In effect, this is expected to reduce the manufacturing costs of Al-12 wt.%Si coatings for low-temperature corrosion-resistant applications. According to Lupoi et al.,[8] in LACS, a laser heats both the substrate and the particles to between 30% and 70% of particle melting point (°C), thereby reducing the particle strength significantly and allowing the particles to deform and build up a coating at an impact velocity lower than those used in CS. A pre-

liminary investigation into the effect of laser power on the LACS deposition mechanism and microstructural evolution of Al-12 wt.%Si coatings is presented in this article. The deposition efficiency, density, microstructure, and microhardness of LACS-deposited coatings produced by a 4.4-kW Nd:YAG laser system were evaluated via optical microscopy (OM) and scanning electron microscopy (SEM).

MATERIALS AND METHODS

Feedstock Powders and Substrate Materials

Gas-atomized Al-12 wt.%Si powders (TLS Technik GmbH, Bitterfield, Germany; +45 μm to 90 μm particle size and distribution) having a near spherical morphology (Fig. 1) was used in this study. The basis for the choice of Al-12 wt.%Si powder having +45 μm to 90 μm range was premised on the fact that this particle size range is typical for cold-spraying powders.[1] Furthermore, they are also cheaper than narrow-band powders. The base material used in this work was 304L stainless steel with dimensions of 100 mm $\times$ 50 mm $\times$ 5 mm. Before powder spraying, the surfaces of base material were roughened by grit blasting to improve the adhesion of the coating to them.

LACS Parameters

The laser-assisted cold-spray equipment used in this study was located at the National Laser Centre/ Council for Scientific and Industrial Research (NLC/ CSIR), Pretoria, South Africa. It included a 4.4-kW Nd:YAG (ROFIN DY 044) laser system of 1.06-μm wavelength and a AT-1200HPHV 500PSI (35-bar) powder feeder (Thermach Inc., Appleton). The converging–diverging (de Laval) DLV-180 nozzle (Centre for Industrial Photonics, Institute for Manufacturing, University of Cambridge, UK under the leadership of Dr. W. O'Neill) employed for spraying the Al-12 wt.%Si particles was mounted on a Kuka robot with the operator controlling the equipment from within the safety enclosure. The Nd:YAG laser system was delivered with a 600-micron step index fiber to a beam-shaping module consisting of a 200-mm focal length (FL) collimator and a Precitec YW50 unit (National Laser Centre, Pretoria, South Africa) fitted with a FL lens. The DLV-180 nozzle having a round exit of 6 mm diameter, expansion ratio of 9, divergent section length of 180 mm, throat diameter of 2 mm, and total length of 210 mm was used for this study.

Al-12 wt.%Si particles were propelled with a high-pressure nitrogen (N_2) gas, which was split and sent to the converging–diverging (de Laval) NDLV nozzle, both directly and via a AT-1200HPHV 500PSI (35-bar) powder feeder, where powder particles were mixed with the gas. Both Al-12 wt.%Si particles and N_2 gas streams then recombined and passed through the nozzle where they were accelerated to supersonic speeds. The

high-velocity, powder-laden jet exited the nozzle and was then directed toward the substrate. The powder stream impacted a region of the substrate that was preheated by the Nd: YAG laser system with the powder stream trailing the laser beam by 15 mm at a time delay of 1.5 s. This arrangement was adopted because Al-12 wt.%Si particles are low-melting-point materials that could easily melt if they were directly exposed to the laser beam.[10] In addition, the spraying nozzle was held perpendicular to the substrate surface while the laser beam was at an angle of 15° to the surface normal (Fig. 2). Laser power was varied between 1.0 kW and 3.5 kW with the gas pressure, powder feed wheel rotation speed, traverse speed, and stand-off distance set at constant values of 12.5 bar, 20 rpm, 10.0 mm/s, and 50.0 mm, respectively. The constant experimental
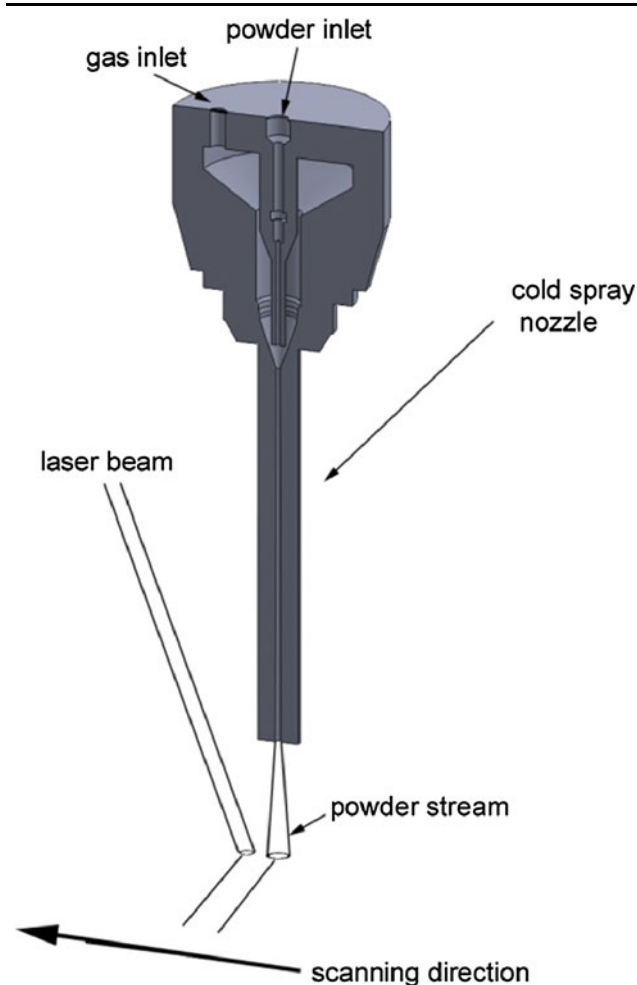

Fig. 2. Layout of LACS system.

Table I. Chemical Composition of Al-12wt.%Si Powders as Determined by EDS

Element	Al	Si	O
wt.% composition	87.23	11.3	1.46

parameters were chosen in line with the manufacturer's suggestions. However, further study will investigate variations in parameters other than laser power. The laser beam had a top hat intensity distribution with an approximate spot size of 5.0 mm. Five layers of LACS Al-12 wt.%Si coatings were deposited for each value of laser power with a single laser pass making up a layer.

Sample Analysis

Cross-sections of the coatings were prepared. The microstructure of each coating was then examined by OM (Olympus BX51 M) and an SEM (JSM5800LV; JEOL Ltd., Tokyo, Japan), coupled with an energy-dispersive spectrometer (EDS). The chemical composition of the feedstock powder was determined by the EDS. The SEM was also used to investigate the microstructure of the coatings and the interfaces between the substrate and the coatings. The chemical composition of the powder, determined by the EDS, is presented in Table I.

The thickness of the coatings was quantitatively measured via the image analysis of optical micrographs. Porosity measurements of coating deposits were also determined by taking optical micrographs of polished cross-sections of samples using the *analySIS FIVE* image analysis software to calculate the area fraction of pores within each image. The microhardness was measured by a Vickers hardness tester (Leitz, Grand Rapids, MI) with a load of 0.1 N and a holding time of 10.0 s. For a better observation of the coating microstructure, some of the polished coatings were etched by Keller's reagent. The effects of laser power on the quality characteristics of the coatings were then studied.

RESULTS

Deposition Efficiency of LACS-Deposited Al-12 wt.%Si Coatings

Deposition efficiency of LACS-fabricated Al-12 wt.%Si coatings at various laser powers is hereby evaluated in respect of the layer thickness of the coatings. Figure 3 shows the cross-sections of the macrostructures of LACS-deposited Al-12 wt.%Si coating at various laser powers. An observation of Fig. 3 reveals that between 1.0 kW and 2.0 kW, thin, discontinuous tracks of coatings were obtained (Fig. 3a–c), whereas at laser powers above 2.0 kW, thick, continuous tracks of coatings were produced (Fig. 3d–f). In addition, it is clear from Fig. 3 that the layer thickness of the deposited coatings increases as the applied laser power increases. This is also corroborated by the measurement of the thickness of the coatings presented in Fig. 4. Figures 3 and 4 also reveal that initially, the increment in the thickness of LACS-deposited Al-12 wt.%Si coatings (22 μm) was not substantial for the laser powers in the range of 1.0 kW to 2.0 kW. However, the increment in thickness of the coating (48 μm)

Deposition Mechanism and Microstructure of Laser-Assisted Cold-Sprayed (LACS) Al-12 wt.%Si Coatings: Effects of Laser Power
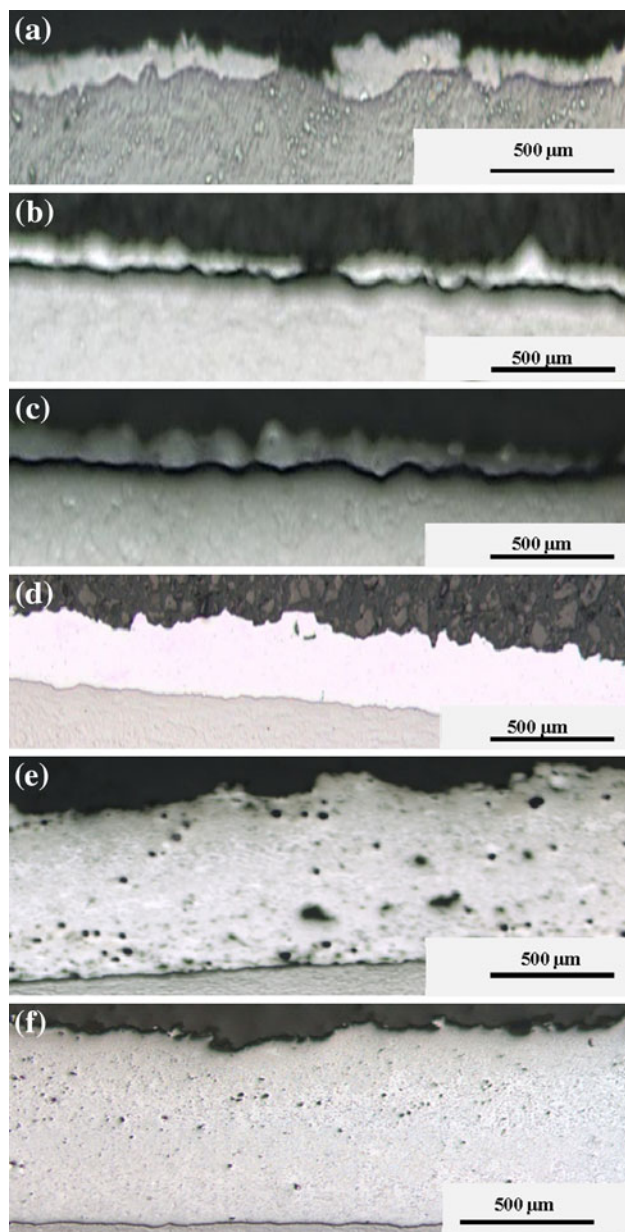
779

Fig. 3. Macrographs of the LACS Al-12 wt.%Si coating samples (deposited on substrates) showing their thicknesses at varying laser powers: (a) 1.0 kW, (b) 1.5 kW, (c) 2.0 kW, (d) 2.5 kW, (e) 3.0 kW, and (f) 3.5 kW.

Fig. 4. Variation of LACS-deposited Al-12 wt.%Si coating thickness with applied laser power.

doubled with the applied laser power increasing from 2.0 kW to 2.5 kW. Four to six times increments in the coating thickness (538 μm to 847 μm) were obtained as the laser power increased from 2.5 kW to 3.5 kW.

Microstructure of LACS-Deposited Al-12 wt.%Si Coatings

Three Al-12 wt.%Si coatings produced by 2.0 kW, 2.5 kW, and 3.0 kW were taken for further microstructural analysis because there occurred a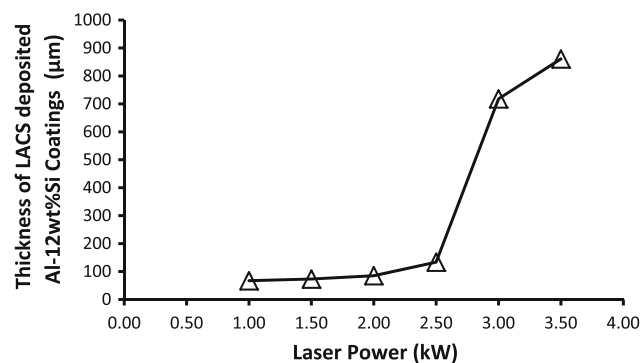 transition in their features at these laser powers as shown in Figs. 3 and 4. An analysis of the etched microstructures of the LACS-deposited Al-12 wt.%Si coatings, by an SEM, indicates that variation in laser power influences alterations in the microstructural characteristics of the coatings (Fig. 5). For example, the coating produced with 2.0 kW was found to be bedevilled with porosity and cracks across its microstructure (Fig. 5a) as well as along its interface with the substrate (Fig. 5d). Moreover, unbonded particles **X** can also be found in this microstructure (Fig. 5a) with its bottom portion noted to be denser than its top portion (Fig. 5a). These unbonded particles compared well to the feedstock powder. This observation suggests that they encountered little or no deformation during LACS processing. A study of Fig. 5b reveals that the LACS-deposited Al-12 wt.%Si coating produced with the 2.5-kW laser power has a well consolidated microstructure. No discernible differences in the cross-section of the microstructure of this coating could be identified as evident by the absence of porosity, cracks, and unbonded particles (Fig. 5b). In addition, the bonding between the coating and the substrate appears to be strong and coherent as no porosity or crack could be located at the interface (Fig. 5e).

With the application of 3.0 kW, the cross-section of coating microstructure (Fig. 5c) was characterized by porosities and cracks. Nevertheless, the coating is noted to be coherently bonded at its interface with the substrate without the existence of cracks and porosities at the interface (Fig. 5f). Figure 5d–f shows the existence of α-Al phase in dark gray with fine silicon cuboids and silicon particulates in light gray contrast in each of the coatings being studied. However, it is pertinent to point out that with an increment in laser power during LACS processing, the larger the regions containing α-Al phase and silicon particulates in the coatings (Fig. 5d–f).

SEM micrograph (Fig. 6) confirms that deformation occurs partly at the top surface of each Al-12 wt.%Si particle by flattening in a manner similar to thermally deposited coatings (see regions PP in
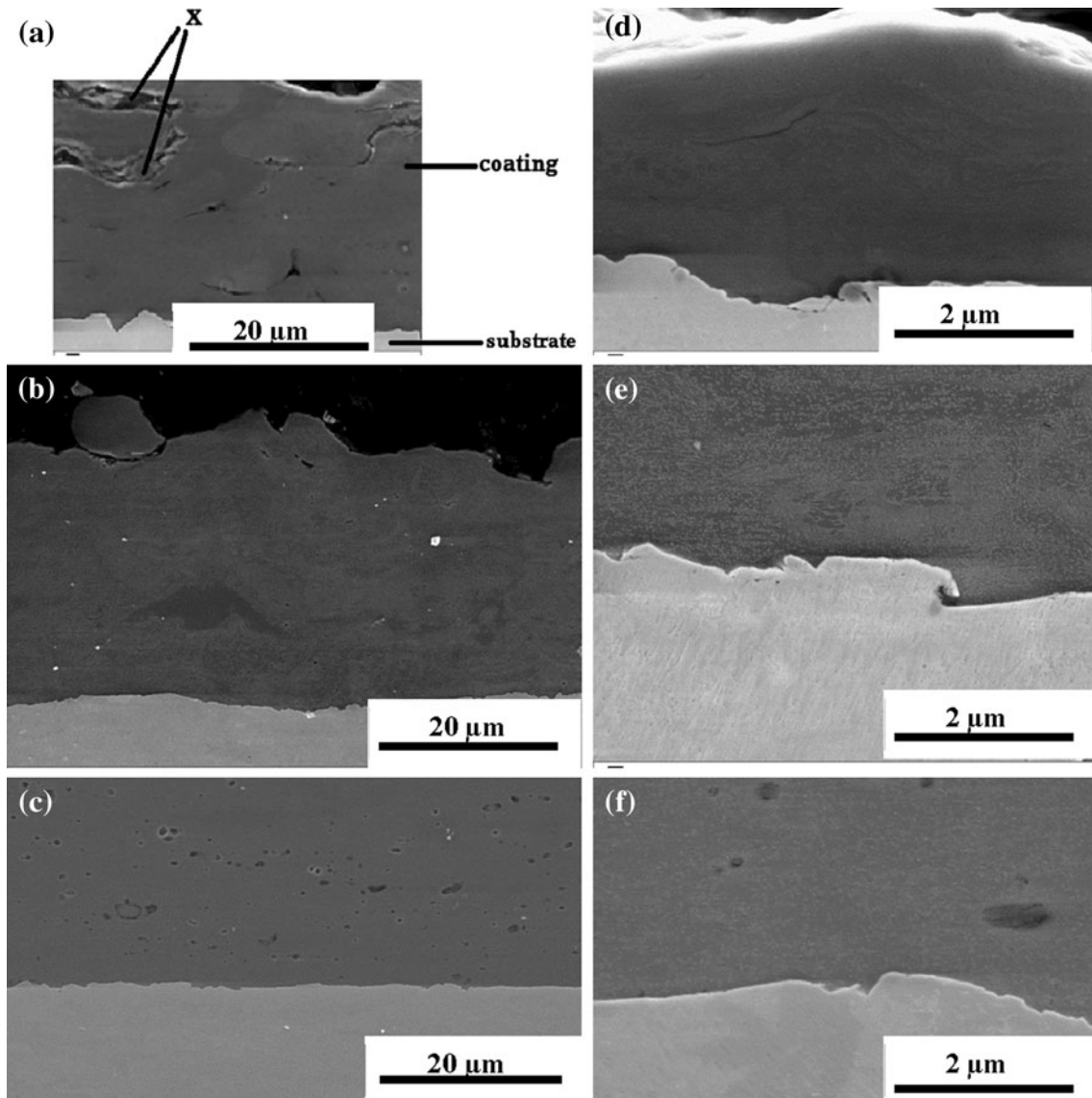
Fig. 5. Microstructures of LACS-deposited Al-12 wt.%Si coatings at varying laser powers (a, d) 2.0 kW, (b, e) 2. 5 kW, and (c, f) 3.0 kW.

Fig. 6) and by forming a coherent layer via melting of Al-12 wt.%Si particles. However, the regions of coherent layer formed by melting are seen to increase as the applied laser power/energy density increases (Fig. 5a–c).

Figure 7 illustrates the porosity measurement for each of the coated samples. It is evident from Fig. 7 that porosity increases in ascending order for the LACS-deposited Al-12 wt.%Si coatings as follows: 2.5 kW < 2.0 kW < 3.0 kW. The porosity analysis (Fig. 7) corroborates the findings from Fig. 5 that coated samples fabricated with 2.0- and 3.0-kW laser powers are much more bedevilled with porosity than the coated sample produced with 2.5 kW laser power.

An analysis of the microhardness results obtained for LACS processed Al-12 wt.%Si coated samples at 2.0, 2.5, and 3.0 kW is presented in Fig. 8 above.

Uniform values of microhardness obtained for the coating produced with 2.5 kW confirms the homogeneity of its microstructure in the absence of porosity or crack (Fig. 8). Nonuniformity in the microhardness profiles of the coatings produced with 2.0 kW and 3.0 kW again lends credence to the claim that porosity and cracks did occur in their microstructures.

DISCUSSION OF RESULTS

Deposition Efficiency of LACS-Deposited Al-12 wt.%Si Coatings

An analysis of the laser beam interaction with the Al-12 wt.%Si powder stream being propelled by cold N_2 gas under high pressure suggests that the laser beam heats up the molecules of the gas. This then results in an increment in its temperature as well as

Deposition Mechanism and Microstructure of Laser-Assisted Cold-Sprayed (LACS) Al-12 wt.%Si Coatings: Effects of Laser Power

781

its kinetic energy in comparison to its cold state before laser irradiation. Consequently, the Al-12 wt.%Si particles also get heated up via the convection process with the attendant effect of an increase in the temperature and kinetic energy of the atoms of the individual particles since they are transported in the already heated N_2 medium. An increment in the kinetic energy of the atoms of the Al-12 wt.%Si particles via the conduction process translates to loosening of their atomic bond energy, which then results in particle softening as their yield strengths are reduced.[9] Moreover, the laser

irradiation also has a softening effect on the deposition site or the substrate via the heat conduction process. This then makes it easier for the Al-12 wt.%Si particles to impact on the deposition site and deform much more easily upon laser irradiation relative to the cold state.[9,10] The increased coating thickness reported in this study as the laser power increases (Figs. 3 and 4) could be attributed to the fact that the Al-12 wt.%Si particles as well as the deposition site become more softened with increased laser power. Therefore, increased softening of both the Al-12 wt.%Si particles and the deposition site lowers their yield strengths for enhanced embedding of the particles on the deposition site. This outcome is similar to the finding by Bray et al.,[9] who deposited commercially pure titanium via LACS.
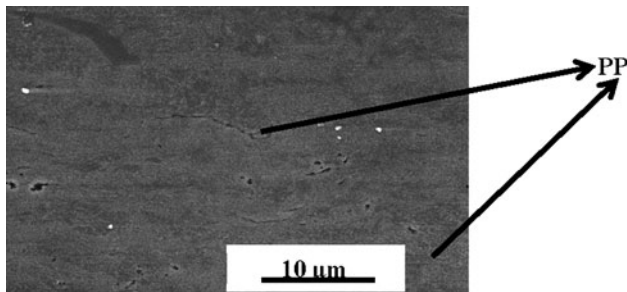
Microstructure of LACS-Deposited Al-12 wt.%Si Coatings

The results obtained from the microstructural analysis of LACS-deposited Al-12 wt.%Si coatings suggest the importance of the appropriate choice of laser power in depositing defect-free coatings. The addition of Si to aluminum alloy prior to atomization promotes the formation of a mullite (Al_2O_3

Fig. 6. Deformation mechanism in LACS-deposited Al-12 wt.%Si coating at 2.5 kW.
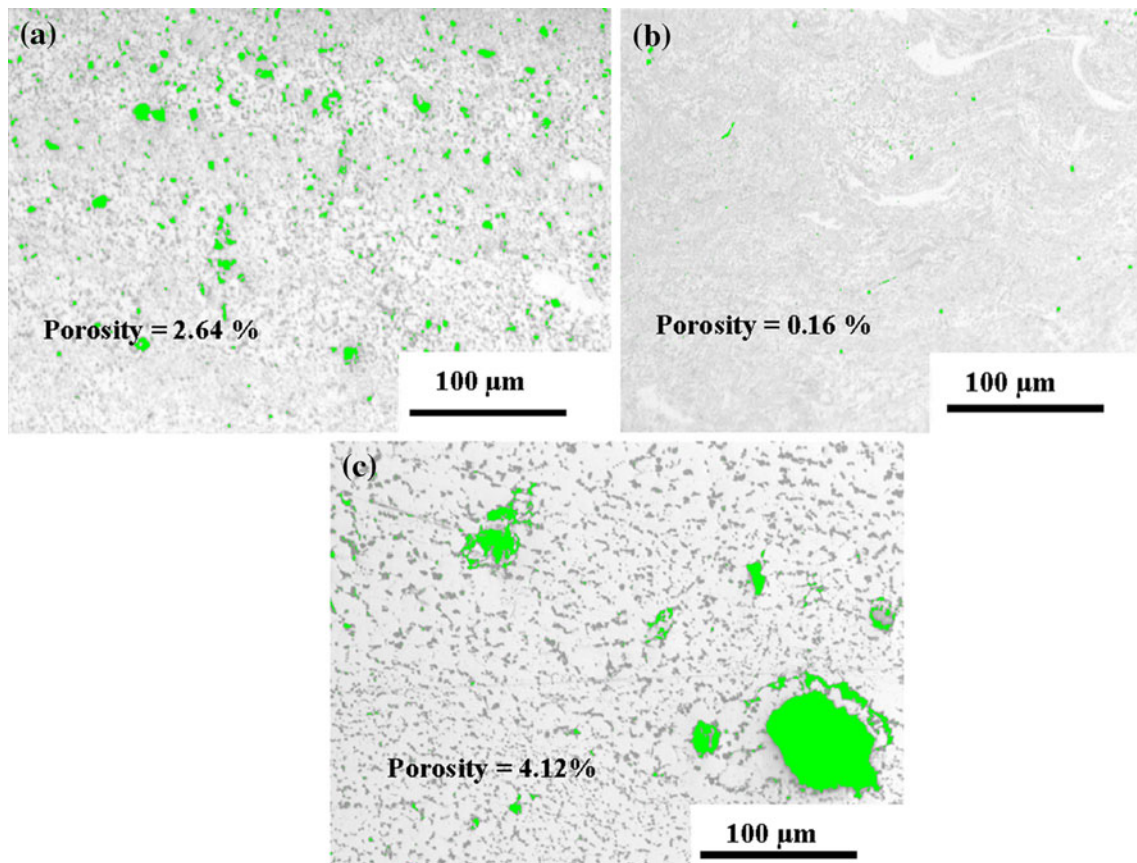

Fig. 7. Porosity analysis in the LACS-deposited Al-12 wt.%Si coatings produced with various laser powers: (a) 2.0 kW, (b) 2.5 kW, and (c) 3.0 kW.
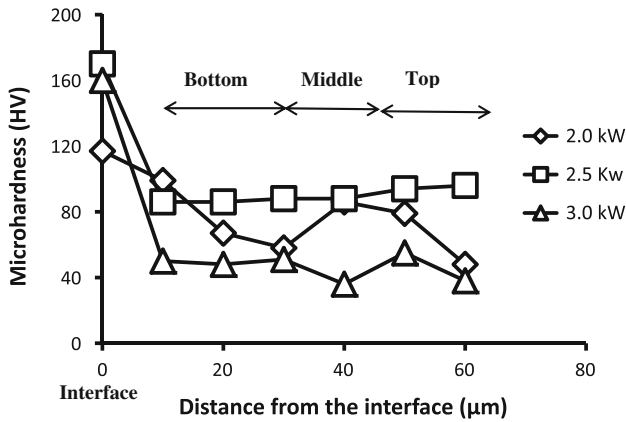
Fig. 8. Microhardness profiles of LACS-deposited Al-12 wt.%Si coatings at 2.0 kW, 2.5 kW, and 3.0 kW.

SiO_2) film that covers the Al-12 wt.%Si particles as reported by Dunkley.[11] According to Olakanmi et al.,[12] the laser irradiation is expected to generate a temperature regime which is sufficiently high to cause the cracking of the mullite film. This occurs so that Al-12 wt.%Si particles could be bonded together upon impacting on the deposition site during LACS processing provided the film thickness is greater than or equal to 0.3 μm and the Al-12 wt.%Si particles are uniformly coated.

The presence of porosity and cracks in the microstructure of the coating produced with 2.0 kW (Fig. 5a) suggests that either the applied laser power is insufficient to cause the cracking of the mullite film covering the Al-12 wt.%Si particles or the thickness of the mullite film is nonuniform or less than 0.3 μm, thereby making interparticulate bonding difficult to be achieved upon impacting the deposition site. This explanation is supported by the presence of unbonded particles in Fig. 5a, porosity measurement (Fig. 7a), as well as the outcome of the microhardness analysis (Fig. 8).

The absence of porosity and cracks in the microstructure of the coating produced with 2.5 kW (Fig. 5b) could be explained by the fact the applied laser power was just sufficient to cause the cracking of the mullite film covering the Al-12 wt.%Si particles. With the mullite film sufficiently cracked upon impacting on the adequately softened deposition site, the softened Al-12 wt.%Si particles effectively bonded to the deposition site and to one another. The absence of unbonded particles in Fig. 5b lends credence to the fact that none of the Al-12 wt.%Si particles has a film thickness less than 0.3 μm or nonuniform since the particle size distribution of the powder under investigation +45 μm to 90 μm. This assertion could be attributed to the absence of smaller sized particles that could have had a thinner mullite film that is difficult to crack or nonuniform thickness. The presence of porosity and cracks in the coating produced with 3.0 kW could be attributed to the increased lifetime of the liquid

phase formation under the given processing conditions,[13] which allowed more time for pore formation due to the nitrogen gas employed to propel the Al-12 wt.%Si particles forming bubbles.

By applying the Rosenthal equation of a moving heat source, the temperature generated for 2.0 kW, 2.5 kW, and 3.0 kW are estimated to be 107°C, 200°C, and 400°C, respectively.[14] With the application of 2.0 kW for the LACS deposition of Al-12 wt.%Si coatings, limited surface melting was observed in Fig. 5a, even though the temperature (107°C) generated by the applied laser power was less than the melting point (577°C) of Al-12 wt.%Si. It may be inferred from Fig. 5a that the temperature rise due to the synergetic effects of adiabatic shearing (I) and laser irradiation (II) of Al-12wt.%Si particles could have exceeded their melting point. This phenomenon is believed to be responsible for the existence of regions containing α-Al phase and silicon particulates in the microstructure of the coating (Fig. 5a). This suggests that supersaturation of α-Al with Si and/or the formation of non-equilibrium phases during rapid solidification of the localized particle interfaces occurred upon the particle impacting on the deposition site. In addition, this region is noted to have existed in all the microstructures irrespective of the applied laser power during the LACS deposition of Al-12 wt.%Si coatings. However, the coating produced with 2.5 kW is noted to contain more regions of limited melting than that produced with 2.0 kW (Fig. 5a and b), while the melted region is very extensive in the coating produced with 3.0 kW (Fig. 5c). The microstructure shown in Fig. 5c is a typical resolidified structure from the melt as observed for the laser sintering of Al-12 wt.%Si alloy.[13] Similar to the finding from Li et al.,[1] the precipitation and/or growth of Si particles occurred in the α-Al matrix during the LACS deposition of Al-12 wt.%Si particles due to the increasing softening effects of the laser power and adiabatic shearing. This then resulted in excess temperature that caused melting of Al-12 wt.%Si. Moreover, the formation of metallurgical bonding between the deposited particles produced with 2.5 kW (Fig. 5b) may be explained by the existence of those limited melting areas considering the relatively high microhardness of the coating. Although the already softened Al-12 wt.%Si particles remained solid during flight, after reaching the deposition site, they encountered high temperatures for a short time. After reaching the deposition site, they encountered high temperatures at the substrate for a limited period of time. This eventually led to their deformation by flattening (see regions PP in Fig. 6) in a manner similar to thermal sprayed coatings.[9] This confirms that the softened Al-12 wt.%Si particles embedded themselves into a heated, cleaned, softened deposition site.[9]

Meanwhile, the degree to which both the Al-12 wt.%Si particles and the substrate are softened is a function of the applied laser power that determines

Deposition Mechanism and Microstructure of Laser-Assisted Cold-Sprayed (LACS)
Al-12 wt.%Si Coatings: Effects of Laser Power

783

the processing temperature as noted earlier on. It is evident from Fig. 5e and f that the temperatures reached at the substrate, when 2.5 kW and 3.0 kW were applied for LACS deposition, weakened the Al-12 wt.%Si particles further, thereby making it easier for them to be embedded on the substrate. The outcome of this phenomenon is the coherent and strong bonding between the coating and the interface of the substrate as suggested by the microhardness values at the interface (Fig. 8). In the case of 2.0 kW (Fig. 5d), the presence of porosity at the interface shows that the applied laser power could not sufficiently soften both the Al-12 wt.%Si particles and the substrate adequately enough to allow effective and coherent bonding of the coating with the substrate (see the interfacial microhardness for the coating sample produced with 2.0 kW).

CONCLUSIONS

The thickness of the LACS-deposited Al-12 wt.%Si coatings increased with increased laser power. Laser power employed for consolidating the coatings influences the possibility of cracking the mullite film covering the Al-12 wt.%Si to effect interparticulate bonding. When depositing the coatings, this occurs via adiabatic shearing as well as thermal softening of the particles. Finally, this study highlights the importance of the appropriate choice of laser power (2.5 kW) in depositing pore- and crack-free Al-12 wt.%Si coatings with strong adhesion to the deposition site by LACS process. Meanwhile, a detailed experimental study employing the Taguchi method of design of experiments to understand the roles of other LACS process parameters in the development and optimization of the coatings is still ongoing.

REFERENCES

1. W.-Y. Li, C. Zhang, X.P. Guo, G. Zhang, H.L. Liao, and C. Coddet, *Appl. Surf. Sci.* 253, 7124 (2007).
2. C. Tekmen, I. Ozdemir, G. Fritsche, and Y. Tsunekawa, *Surf. Coat. Technol.* 203, 2046 (2009).
3. B. Torres, M. Campo, and J. Rams, *Surf. Coat. Technol.* 203, 1947 (2009).
4. R. Anandkumar, A. Almeida, and R. Vilar, *Wear* 282–283, 31 (2012).
5. L. Zhao, K. Bobzin, D. He, J. Zwick, F. Ernst, and E. Lugscheider, *Adv. Eng. Mater.* 8, 264 (2006).
6. J. Wu, J. Yang, H. Fang, S. Yoon, and C. Lee, *Appl. Surf. Sci.* 252, 7809 (2006).
7. M. Yandouzi, P. Richer, and B. Jodoin, *Surf. Coat. Technol.* 203, 3260 (2009).
8. R. Lupoi, M. Sparkes, A. Cockburn, and W. O'Neill, *Mater. Lett.* 65, 3205 (2011).
9. M. Bray, A. Cockburn, and W. O'Neill, *Surf. Coat. Technol.* 203, 2851 (2009).
10. D.K. Christoulis, S. Guetta, E. Irissou, V. Guipont, M.H. Berger, M. Jeandin, J.-G. Legoux, C. Moreau, S. Costil, M. Boustie, Y. Ichikawa, and K. Ogawa, *J. Therm. Spray Technol.* 19, 1062 (2010).
11. J.J. Dunkley, *Powder Metal Technologies and Applications* (Materials Park, OH: ASM International, 1998), pp. 35–52.
12. E.O. Olakanmi, R.F. Cochrane, and K.W. Dalgarno, *TMS2009 Supplemental Proceedings: Volume I: Materials Processing and Properties* (Warrendale, PA: TMS, 2009), pp. 371–380.
13. E.O. Olakanmi, R.F. Cochrane, and K.W. Dalgarno, *J. Mater. Process. Technol.* 211, 113 (2011).
14. K.E. Easterling, *Introduction to the Physical Metallurgy of Welding*, 2nd ed. (Oxford, U.K.: Butterworth-Heinemann Ltd., 1992).